THE JOURNAL OF PHYSICAL CHEMISTRY C LETTERS

2009, *113,* 14067–14070
Published on Web 07/17/2009

Time-Domain Ab Initio Study of Nonradiative Decay in a Narrow Graphene Ribbon

Bradley F. Habenicht and Oleg V. Prezhdo*

Department of Chemistry, University of Washington, Seattle, Washington 98195-1700

Received: May 27, 2009; Revised Manuscript Received: July 6, 2009

We investigate nonradiative decay in the (16,16) armchair graphene nanoribbon (GNR) using surface-hopping with decoherence in a time-dependent Kohn−Sham scheme. The lowest singlet excitation decays within 300 ps in the ideal GNR by coupling to the 1450 cm^{-1} disorder mode associated with edges. The C_2-insertion defect doubles the decay rate. Compared to carbon nanotubes (CNTs), GNRs are more anharmonic and show faster phonon-induced pure dephasing of electronic transitions. Defects relieve strain better and, therefore, exhibit weaker electron−phonon coupling in GNRs than CNTs. The slower nonradiative decay of GNRs compared to similar size CNTs makes GNRs better candidates for the semiconductor applications.

The isolation of a single atomic layer of graphite, or a graphene sheet, in 2004[1] instigated global efforts to study the synthesis, features, and device applications of this quasi-two-dimensional structure.[2] The intense interest has led to the discovery of new physical properties,[3−5] improved fabrication techniques,[6] and proof-of-concept transistors[7] and transparent liquid-crystalline films.[8] Following graphene sheets, graphene nanoribbons (GNR) were synthesized.[9,10] The quantum confinement and edge effects created in GNRs by reduced dimensionality generate novel properties[10−16] and diversify the range of applications, including logic gates and field-effect transistors,[17,18] spin filters[19] and spintronic devices,[20] optical and conductance switches,[21] and photovoltaic systems and superconductors.[22] Many of these applications rely on the dynamics of charges and excitations, which strongly interact with phonons, as shown already for the closely related carbon nanotube (CNT) systems both with optical experiments[23−28] and theory.[29−35] For instance, charge−phonon interactions result in energy losses and heating in nanoelectronic and photovoltaic applications. Similarly, spin−phonon interactions are responsible for coherence loss in spintronic devices. At the same time, fast electron-vibrational relaxation to the ground state is key for optical and conductance switches, since it determines the switch response time. The electron−phonon interaction provides an electron-pairing mechanism in nanoribbon superconductors. Therefore, it becomes essential, on both fundamental and practical sides, to study electron−phonon dynamics in GNRs and to provide insights into the photophysics of this material.

In this Letter, we probe the fundamental mechanisms of electron−phonon relaxation in a narrow GNR with and without defects, using a state-of-the-art time-domain atomistic simulation. The first study of this kind, it reveals a number of unforeseen features of electron−phonon dynamics in GNRs compared to similar-size CNTs. In particular, in spite of the smaller excitation energy, the lowest energy singlet excitations decay more slowly in the GNRs due to weaker nonadiabatic (NA) coupling and smaller Franck−Condon factors. The relaxation of the ideal ribbon is induced primarily by the disorder mode near 1450 cm^{-1} associated with the edges, rather than by the 1600 cm^{-1} carbon stretching mode typical of CNTs, conjugated polymers, and molecular systems.[34,36] Similarly to CNTs, defects accelerate the nonradiative decay. The acceleration is less significant, however, because defects are able to relieve the geometric strain by deforming GNRs. Phonon motions are more anharmonic in GNRs than CNTs. As a result, phonon-induced pure dephasing of electronic excitations occurs faster in GNRs than CNTs, even though the phonon-induced energy decay is slower. Further, the GNR defect accelerates relaxation but slows pure dephasing. This is in contrast to CNTs, in which defects accelerate both relaxation and dephasing. The slower nonradiative decay and longer lifetimes of electronic excitations in GNRs compared to CNTs make GNRs better candidates for the semiconductor applications.

The simulation utilizes the quantum-classical fewest-switches surface-hopping (FSSH) technique[37] implemented within the time-dependent Kohn−Sham (TDKS) scheme[38] and including the semiclassical correction for quantum decoherence.[35,39] The method and related approaches were used previously to model electron−phonon relaxation in CNTs,[33,35] quantum dots,[40] semiconductor interfaces,[41] and biological systems.[38] The approach provides a detailed ab initio picture of the relaxation dynamics at the atomistic level and in time-domain. The FSSH-TDKS theory was implemented within the Vienna ab initio simulations package.[42] The electronic structure was obtained using a converged plane-wave basis, the Perdew−Wang generalized gradient approximation,[43] and projector-augmented-wave pseudopotentials.[44] The more advanced treatments of electronic excitations, e.g., Bethe−Salpeter[45] and multiconfiguration[46] approaches, and phonon dynamics, e.g., multiconfiguration Hartree[47] and quantized Hamilton dynamics,[48] are too computationally expensive for the present systems.

The (16,16) armchair GNR was chosen for the present study, Figure 1. The GNR was cut from an infinite layer of graphene. The dangling bonds at the edges were saturated with hydrogen atoms. The GNR geometry was fully relaxed using the standard VASP procedures and including optimization of both the unit cell size in the periodic dimension and atomic coordinates.

* Corresponding author. E-mail: prezhdo@u.washington.edu.

10.1021/jp904937c CCC: $40.75

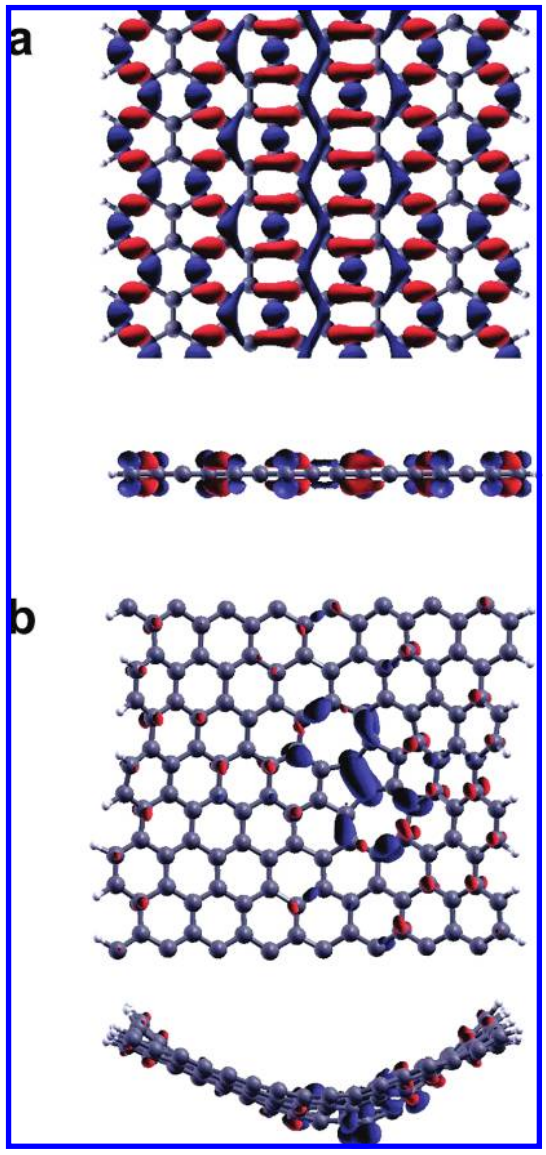

Figure 1. Geometric structure and transition density of the lowest energy excitation in (a) ideal (16,16) GNR and (b) (16,16) GNR with the 7557 defect. Top and side views are presented for each GNR. Carbon atoms are gray, and hydrogen atoms are white. Red and blue colors correspond to positive and negative changes in electron density.

Periodic boundary conditions were used along the length of the GNR, and 8 Å of vacuum were included in the directions perpendicular to the ribbon length to avoid fictitious interactions. Following geometry optimization, the systems were brought up to room temperature by repeated velocity rescaling. Then, microcanonical trajectories were run in the ground electronic state. The initial conditions for the TDKS-FSSH simulations were sampled from these trajectories.

To investigate the effect of disruptions to the hexagonal lattice, the 7557 defect was introduced. It involves insertion of a C−C dimer into the lattice hexagon, creating two five- and two seven-membered rings. The defect alters both the electronic and geometric structure of the GNR, Figure 1b. It causes an out-of-plane buckling of the lattice and creates a strongly localized electronic transition with the excitation energy below that of the ideal ribbon, Table 1.

Figure 2 presents a 1 ps long trajectory of the first excitation energies for the ideal (16,16) GNR and the GNR with the 7557 defect. The defect lowers the excitation energy, as expected.

TABLE 1: Average Excitation Energy, Absolute Value of NA Coupling, Pure Dephasing Time, and Relaxation Time for the Ideal (16,16) GNR and the 7557 Defect

GNR	excitation (eV)	coupling[a] (meV)	dephasing (fs)	relaxation (ps)
ideal	0.76 ± 0.079	0.92 ± 1.3	24	309
7557	0.59 ± 0.045	1.2 ± 1.6	42	124

[a] The large standard deviation indicates large fluctuations in the coupling magnitude, which remains positive by definition.

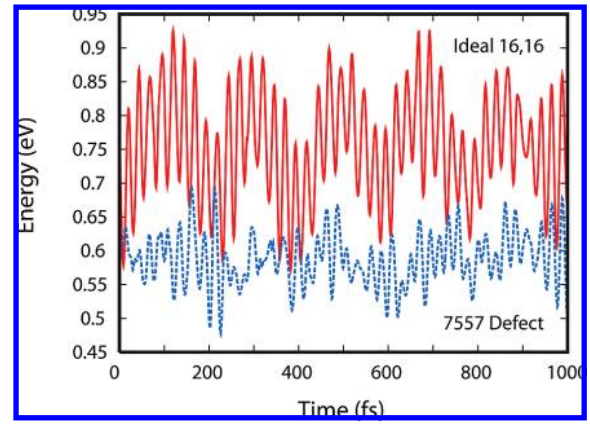

Figure 2. Fluctuation of the lowest excitation energy due to phonon motions for the ideal (16,16) GNR, red solid line, and (16,16) GNR with the 7557 defect, dashed blue line.

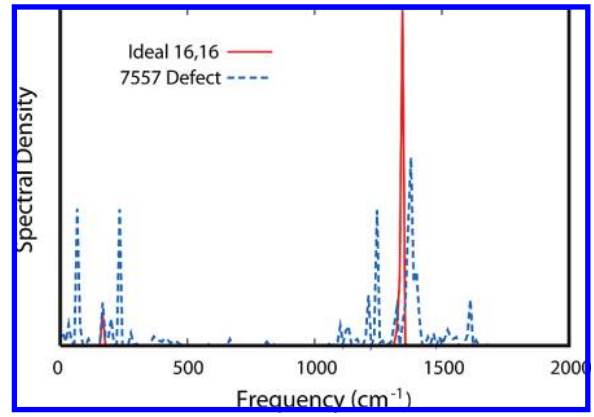

Figure 3. Fourier transforms of the autocorrelation functions of the excitation energies shown in Figure 2. The data for the 7557 defect are multiplied by 30. The excitation in the ideal GNR couples primarily to the disorder mode near 1450 cm^{-1} as well as to an acoustic mode near 200 cm^{-1} that is similar in frequency to radial breathing modes in CNTs. The defect couples to a wide range of atomic motions.

The energy fluctuation is notably smaller for the defect than the ideal GNR. This is in contrast to CNTs,[35] which showed a slightly larger oscillation of the defect energy relative to the ideal tube. The difference arises from the phonon properties of the ideal GNR and CNT rather than defects, which are roughly similar in the two materials. Less stiff than CNTs, GNRs move with a larger amplitude. The energy fluctuations seen in the defected GNR are more random than those in the ideal ribbon. This result is verified by the Fourier transforms (FT) of the autocorrelation functions of the excitation energy, Figure 3. The FT were obtained on the basis of the microcanonical ground state trajectories. A much wider range of phonon modes is seen with the defect than the ideal GNR. The latter couples almost exclusively to the disorder mode near 1450 cm^{-1}, which has been detected experimentally near the edges of single graphene sheets.[5] A weak signal is seen from the radial breathing-like

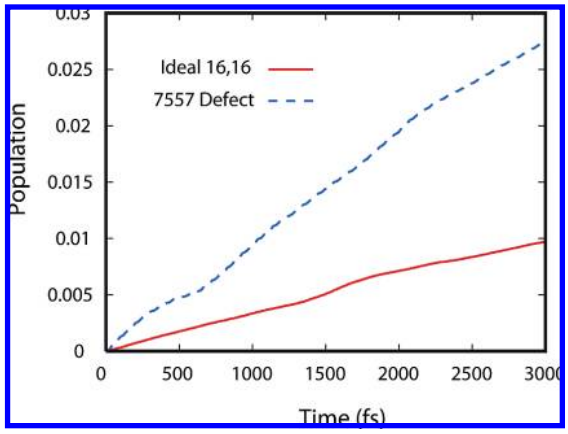

Figure 4. Recovery of the ground state population due to nonradiative relaxation of the lowest energy excited state as a function of time in the GNRs studied.

mode near 200 cm^{-1} [15] as well. The phonon spectral density of the defected GNR is an order of magnitude smaller than that of the ideal GNR, indicating that the local modes induced by the defect do not affect the electronic system as much as the disorder mode. The range of modes available to the defect in GNR is broader than in CNT,[35] in which the defect couples primarily to a single mode at the radial breathing frequency. By distorting the ribbon, the defect is able to involve many of the ribbon modes.

The recovery of the ground state population via the nonradiative decay of the lowest excited state is shown in Figure 4. By assuming that the nonradiative decay is exponential, as has been determined in CNTs,[26−28] the simulation data are fit using the relation $P(t) = 1 - \exp(t/\tau) \approx t/\tau$. The relaxation times τ are shown in Table 1.

Comparing the nonradiative relaxation in the ideal GNR to that with the 7557 defect, we observe that the defect speeds up the relaxation by approximately 2.5. This is due to three factors. First, the smaller excitation energy requires fewer phonon quanta to redistribute the energy to the lattice. Second, the defect localizes the phonon modes and the electronic excitation, Figure 1b, generating stronger NA coupling, Table 1. Third, the longer pure dephasing time of the defect corresponds to a larger Franck−Condon factor, since the latter is the time-domain equivalent of the dephasing/decoherence.[39] The first two factors are the same in CNTs.[35] However, pure dephasing proceeds differently in tubes and ribbons. The 1450 cm^{-1} GNR disorder mode is more anharmonic than the 1600 cm^{-1} C−C stretching mode prominent in CNTs. As a result, pure dephasing is faster in the ideal GNR than in the ideal CNT. In contrast, the 7557 defect is more harmonic in the ribbon than in the tube, because it is able to relieve the geometric strain by deforming the ribbon, Figure 1b. Correspondingly, the phonon-induced pure dephasing of the electronic excitation localized on the defect proceeds more slowly in the GNR than the CNT.

Comparing the nonradiative relaxation in the GNRs and similar size CNTs,[35] we observe that the excited state lifetime predicted for the GNR in the current work is approximately twice as long as that for the CNTs. This is despite the fact that the excitation energy of the CNTs is nearly twice larger than in the GNR. The tube decays faster because of the larger NA coupling and longer pure dephasing, i.e., larger Franck−Condon factor. The NA coupling in both materials is created by the overlap of the π-electron orbitals that extend perpendicularly to the plane of the atoms. CNT curvature brings one side of the π-lobes closer together and increases the overlap. Thus, the NA coupling is stronger in CNTs than in GNRs. On the other hand, the phonon-induced pure dephasing of the electronic transitions is slower in tubes than ribbons. Since ribbons are more flexible than tubes, electronic excitations of GNRs create larger geometric distortions, resulting in increased Stokes' shifts, broader Franck−Condon progressions, wide lines, and faster pure dephasing. The fact that the dephasing in GNRs is facilitated by the anharmonic disorder mode, Figure 3, favors faster dephasing as well.

The magnitude of the NA coupling depends on the overlap of the π-electron orbitals, and therefore, it should decrease with increasing CNT diameter and decreasing curvature. On the other hand, all GNRs are relatively flat, and the overlap argument does not apply. The NA coupling may depend on the ribbon chirality. For instance, zigzag ribbons have localized edge states[11] that are qualitatively different from the delocalized states of the armchair ribbons, Figure 1a. Generally, localized states create larger electron−phonon coupling. The NA coupling and other properties of localized states are relatively independent of the ribbon width, while delocalized states show strong width dependence. In particular, theoretical analyses of armchair GNRs showed strong width dependence of the band gap energy.[12,13] Therefore, one may expect that fluorescence studies on ensembles of GNRs should show a broad distribution of lifetimes even for ribbons of similar widths, due to the variation of the excited state properties with ribbon chirality.

Our simulations predict that excited electronic states of narrow GNRs decay nonradiatively within hundreds of picoseconds. The results generated previously with this technique for CNTs were in good agreement with experiments.[33,35] As the simulation was carried out in a vacuum, our results should be compared to suspended GNRs.[9] Interactions with substrate can provide additional nonradiative decay channels and affect the pure dephasing time. Our simulation assumes that the ground state recovery occurs from the lowest energy singlet excited state. The assumption is based on the fact that the decay of higher energy singlet excitations to the lowest excitation is fast. The recent study on the ultrafast carrier dynamics in graphene showed that hot carriers relax through the (quasi-)continuum of electronic states within several picoseconds,[49] helping to validate the assumption. It should be noted that the extremely small spin−orbit coupling predicted for graphene[50] makes the nonradiative decay by intersystem crossing to the triplet manifold unlikely.

In conclusion, we have investigated the nonradiative decay of excited electrons in a narrow graphene ribbon with and without a common defect. The lowest excited state in the GNR decays in approximately 300 ps, or about half as quickly as in small diameter CNTs. The 7557 defect creates a local geometric distortion to the lattice and increases the decay rate by a factor of 2. The nonradiative relaxation occurs primarily via the disorder mode near 1450 cm^{-1} in the ideal GNR and by a wide range of modes in the defected GNR. Since all GNRs should have approximately the same NA coupling due to lack of curvature, the nonradiative decay time should scale directly with the excitation energy.

References and Notes

(1) Novoselov, K. S.; Geim, A. K.; Morozov, S. V.; Jiang, D.; Zhang, Y.; Dubonos, S. V.; Grigorieva, I. V.; Firsov, A. A. *Science* **2004**, *306*, 666.

(2) Geim, A. K.; Novoselov, K. S. *Nat. Mater.* **2007**, *6*, 183.

(3) Zhang, Y. B.; Tan, Y. W.; Stormer, H. L.; Kim, P. *Nature* **2005**, *438*, 201.

(4) Berger, C.; Song, Z. M.; Li, X. B.; Wu, X. S.; Brown, N.; Naud, C.; Mayou, D.; Li, T. B.; Hass, J.; Marchenkov, A. N.; Conrad, E. H.; First, P. N.; de Heer, W. A. *Science* **2006**, *312*, 1191.

(5) Ferrari, A. C.; Meyer, J. C.; Scaradaci, V.; Casiraghi, C.; Lazzeri, M.; Mauri, F.; Piscanec, S.; Jiang, D.; Novoselov, K. S.; Roth, S.; Geim, A. K. *Phys. Rev. Lett.* **2006**, *97*, 187401.
(6) Dato, A.; Radmilovic, V.; Lee, Z. H.; Phillips, J.; Frenklach, M. *Nano Lett.* **2008**, *8*, 2012.
(7) Berger, C.; Song, Z. M.; Li, T. B.; Li, X. B.; Ogbazghi, A. Y.; Feng, R.; Dai, Z. T.; Marchenkov, A. N.; Conrad, E. H.; First, P. N.; de Heer, W. A. *J. Phys. Chem. B* **2004**, *108*, 19912.
(8) Blake, P.; Brimicombe, P. D.; Nair, R. R.; Booth, T. J.; Jiang, D.; Schedin, F.; Ponomarenko, L. A.; Morozov, S. V.; Gleeson, H. F.; Hill, E. W.; Geim, A. K.; Novoselov, K. S. *Nano Lett.* **2008**, *8*, 1704.
(9) Meyer, J. C.; Geim, A. K.; Katsnelson, M. I.; Novoselov, K. S.; Booth, T. J.; Roth, S. *Nature* **2007**, *446*, 60.
(10) Li, X.; Wang, X.; Zhang, L.; Lee, S.; Dai, H. *Science* **2008**, *319*, 1229.
(11) Nakada, K.; Fujita, M.; Dresselhaus, G.; Dresselhaus, M. S. *Phys. Rev. B* **1996**, *54*, 17954.
(12) Barone, V.; Hod, O.; Scuseria, G. E. *Nano Lett.* **2006**, *6*, 2748.
(13) Son, Y. W.; Cohen, M. L.; Louie, S. G. *Phys. Rev. Lett.* **2006**, *97*, 216803.
(14) Yang, L.; Park, C. H.; Son, Y. W.; Cohen, M. L.; Louie, S. G. *Phys. Rev. Lett.* **2007**, *99*, 186801.
(15) Zhou, J.; Dong, J. *Appl. Phys. Lett.* **2007**, *91*, 173108.
(16) Wimmer, M.; Adagideli, I.; Berber, S.; Tomanek, D.; Richter, K. *Phys. Rev. Lett.* **2008**, *100* (17), 177207.
(17) Wang, X.; Ouyang, Y.; Li, X.; Wang, H.; Guo, J.; Dai, H. *Phys. Rev. Lett.* **2008**, *100* (20), 206803.
(18) Liang, G.; Neophytou, N.; Lundstrom, M. S.; Nikonov, D. E. *Nano Lett.* **2008**, *8* (7), 1819−1824.
(19) Martins, T. B.; da Silva, A. J. R.; Miwa, R. H.; Fazzio, A. *Nano Lett.* **2008**, *8* (8), 2293−2298.
(20) Kim, W. Y.; Kim, K. S. *Nature Nanotech.* **2008**, *3* (7), 408−412.
(21) Cresti, A. *Nanotechnology* **2008**, *19* (26), 265401.
(22) Liang, Q.; Dong, J. *Nanotechnology* **2008**, *19* (35), 355706.
(23) Huang, L.; Pedrosa, H. N.; Krauss, T. D. *Phys. Rev. Lett.* **2004**, *93*, 017403.
(24) Htoon, H.; OConnell, M. J.; Doorn, S. K.; Klimov, V. I. *Phys. Rev. Lett.* **2005**, *94*, 127403.
(25) Wang, F.; Dukovic, G.; Brus, L. E.; Heinz, T. F. *Science* **2005**, *308*, 838.
(26) Wang, F.; Dukovic, G.; Brus, L. E.; Heinz, T. F. *Phys. Rev. Lett.* **2004**, *92*, 177401.
(27) Ma, Y.-Z.; Valkunas, L.; Bachilo, S. M.; Fleming, G. R. *Phys. Chem. Chem. Phys.* **2006**, *8*, 5689.
(28) Jones, M.; Metzger, W. K.; McDonald, T. J.; Engtrakul, C.; Ellingson, R. J.; Rumble, G.; Heben, M. J. *Nano Lett.* **2007**, *7*, 300.
(29) Perebinos, V.; Tersoff, J.; Avouris, P. *Phys. Rev. Lett.* **2005**, *94*, 086802.
(30) Barone, V.; Peralta, J. E.; Wert, M.; Heyd, J.; Scuseria, G. E. *Nano Lett.* **2005**, *5*, 1621.
(31) Tretiak, S. *Nano Lett.* **2007**, *7*, 2201.
(32) Tretiak, S.; Kilina, S.; Piryatinski, A.; Saxena, A.; Martin, M. L.; Bishop, A. R. *Nano Lett.* **2007**, *7*, 86.
(33) Habenicht, B. F.; Craig, C. F.; Prezhdo, O. V. *Phys. Rev. Lett.* **2006**, *96*, 187401.
(34) Habenicht, B. F.; Kamisaka, H.; Yamashita, K.; Prezhdo, O. V. *Nano Lett.* **2007**, *7*, 3260.
(35) Habenicht, B. F.; Prezhdo, O. V. *Phys. Rev. Lett.* **2008**, *100*, 197402.
(36) Schwartz, B. J. *Annu. Rev. Phys. Chem.* **2003**, *54*, 141.
(37) Tully, J. C. *J. Chem. Phys.* **1990**, *93*, 1061.
(38) Craig, C. F.; Duncan, W. R.; Prezhdo, O. V. *Phys. Rev. Lett.* **2005**, *95*, 163001.
(39) Prezhdo, O. V.; Rossky, P. J. *J. Chem. Phys.* **1997**, *107*, 5863.
(40) Kilina, S. V.; Craig, C. F.; Kilin, D. S.; Prezhdo, O. V. *J. Phys. Chem. C* **2007**, *111*, 4871.
(41) Duncan, W. R.; Craig, C. F.; Prezhdo, O. V. *J. Am. Chem. Soc.* **2007**, *129*, 8528.
(42) Kresse, G.; Furthmüller, J. *Comput. Mater. Sci.* **1996**, *6*, 15–50.
(43) Perdew, J. P.; Burke, K.; Wang, Y. *Phys. Rev. B* **1996**, *54*, 16533.
(44) Kresse, G.; Joubert, D. *Phys. Rev. B* **1999**, *59*, 1758.
(45) Yang, L.; Cohen, M. L.; Louie, S. G. *Nano Lett.* **2007**, *7*, 3112.
(46) Isborn, C. M.; Prezhdo, O. V. *J. Phys. Chem. C*, in press.
(47) Wang, H. B.; Thoss, M. *J. Chem. Phys.* **2003**, *119*, 1289.
(48) Prezhdo, O. V. *Theor. Chem. Acc.* **2006**, *116*, 206.
(49) Dawlaty, J. M.; Shivaraman, S.; Chandrashekhar, M.; Rana, F.; Spencer, M. G. *Appl. Phys. Lett.* **2008**, *92*, 042116.
(50) Huertas-Hernando, D.; Guinea, F.; Brataas, A. *Phys. Rev. B* **2006**, *74*, 155426.

JP904937C